

Power efficient control algorithm of electromechanical unbalance vibration exciter with induction motor

V V Topovskiy, G M Simakov

Novosibirsk State Technical University, 20, Karla Marksa Av., Novosibirsk, 630073, Russia

E-mail: topovskij.2013@corp.nstu.ru

Abstract. A control algorithm of an electromechanical unbalance vibration exciter that provides a free rotational movement is offered in the paper. The unbalance vibration exciter control system realizing a free rotational movement has been synthesized. The structured modeling of the synthesized system has been carried out and its transients are presented. The advantages and disadvantages of the proposed control algorithm applied to the unbalance vibration exciter are shown.

1. Introduction

Nowadays, vibrotechnics is widely used in a seismic exploration, mechanical engineering, transport, vibration stands, construction and for a vibration isolation of structures, machines, devices and people.

A typical example of vibrotechnics used in a seismic exploration is an electromechanical unbalance vibration exciter. In comparison with the more common method of seismic surveys such as explosions, a seismic vibration has a lot of advantages - safety at work, smaller damage of nature, as well as controllability of the generated oscillations.

Despite the fact that in devices, such as electromechanical unbalance vibration exciters, direct current motors (DC motors) are usually used, the applying of vector control principles allows us to control squirrel-cage induction motors as easy as it is in the case of a separately excited DC motor.

Unbalance vibration exciters operates by the following principle – two unbalanced masses or eccentrics are fixed on the rods and they rotates relative to the shafts of the two paired semimodules. The semimodules are mounted on the common platform (often called radiant); each of them has an individual drive motor. Rotation of the eccentrics is carried out synchronously and in phase in opposite directions in order to compensate the transverse components of centrifugal forces, and vertical components will be of the same direction in that case. As a result, a vertically polarized excitation force is generated and it affects the platform and, hence, the ground [1].

The unbalance vibration exciters principle of operation and design features are the reasons for the specific characteristics of electric drives for such devices [2]. These are a big inertia moment of the electric drive's rotating masses and a load torque as a sinusoidal function of the unbalanced mass rotation angle.

Harmonicity of the load entails undesirable oscillations of the induction motor's q-axis current component in the quasi-steady mode. This, in turn, leads to the increase of the heat loss in electric drive power circuit and deterioration of its energy characteristics. Thus, one of the most important problems in the control of electromechanical unbalance vibration exciters is a current ripple level



reduction.

In this way, the task to the synthesize control algorithm that realizes the free rotational movement of the unbalances is defined since in this case, the engine torque overcomes only the frictional torque, and the current fluctuations practically absent [3].

In order to show the implementability of such control algorithm, one must first examine the nature of electric drive's load. It can be represented as the sum of two components, one of which caused by the gravity acting on the unbalances, and the other — by the friction force in the unbalances support bearings [4]. Obviously, a classical automatic control system (e.g., cascade control system) will try to maintain the speed at a given level, and, hence it will generate current pulsations during the entire period of operation. If the control of a vibration exciter will be realized so that, when speed will reach its given value, the engine torque will become equal to the frictional torque, a free rotational movement of the unbalances will take place, and the current pulsations will be minimized.

2. Problem definition

In this paper, the following tasks are set. The first one is to deduce the electric drive's control law providing a free rotational movement of the eccentric. The second one lies in synthesizing the vector control system with the proposed control law, paying attention to the mathematical model of the pre-magnetized induction motor. It is also necessary to achieve the correspondence of the seismic signal amplitude and its frequency to the required values when calculating system's parameters. One of the tasks consists in structured modeling of the synthesized control system, which follows after that calculation of its dynamic characteristics. In order to show the advantages of the proposed control law, the final goal is to compare the synthesized control system with the cascade control system, which has the same parameters of the power unit.

3. Theory

Considering the above-mentioned, load torque of the vibration exciter, the electric drive can be written as:

$$T_L = T_{FR} + mgr \sin \varphi$$

where T_{FR} – frictional torque in bearing; m – mass of the eccentric; g – acceleration of gravity; r – rotation radius of the eccentric; φ – rotation angle of the eccentric.

Then the motion equation of the unbalance vibration exciter electric drive can be represented as follows [5]:

$$J_{\Sigma} \frac{d\omega}{dt} = T - T_{FR} - mgr \sin \varphi,$$

where J_{Σ} – total inertia moment of the drive reduced to the motor shaft; ω – rotational speed of the eccentric; T – engine torque.

If a friction compensation ($T = T_{FR}$) is achieved in the quasi-steady mode, the motion equation of the drive will change as follows:

$$J_{\Sigma} \frac{d\omega}{dt} = -mgr \sin \varphi.$$

Dividing both sides of the equation by $\omega = d\varphi / dt$, one obtains the following equation:

$$J_{\Sigma} \omega d\omega = -mgr \sin \varphi d\varphi.$$

Integrating both sides of the equation, one gets:

$$J_{\Sigma} \frac{\omega^2}{2} = mgr \cos \varphi + C_1.$$

Hence, one obtains the desired law of speed variation:

$$\omega(\varphi) = \left(\frac{2}{J_{\Sigma}} mgr \cos \varphi + C_1 \right)^{1/2}.$$

Let us find integration constant C_1 under the following initial conditions $\varphi = 0$, $\omega = \omega_0$ [6]:

$$C_1 = \omega_0^2 - \frac{2}{J_{\Sigma}} mgr.$$

Finally, the desired law of speed variation takes the following form:

$$\omega(\varphi) = \left[\frac{2}{J_{\Sigma}} mgr (\cos \varphi - 1) + \omega_0^2 \right]^{1/2}.$$

To implement such relationship $\omega(\varphi)$, the control law ($U_{\omega}^{ref}(t)$) can be approximated as:

$$U_{\omega}^{ref}(t) \approx k_{\omega} \omega = k_{\omega} \left[\frac{2}{J_{\Sigma}} mgr (\cos \varphi - 1) + \omega_0^2 \right]^{1/2}. \quad (1)$$

Let us establish relation of the value ω_0 with the frequency of the generated seismic signal Ω .

In order to do that, one has to find rotational speed of the eccentric at the upper point of its path [7], when $\varphi = \pi$:

$$\omega_1 = \sqrt{\omega_0^2 - \frac{4}{J_{\Sigma}} mgr}.$$

Frequency of the seismic vibrations can be approximately written as the average speed of the eccentric:

$$\Omega = \frac{\omega_1 + \omega_0}{2}.$$

As a result, after the substitution and transformations, one obtains:

$$\omega_0 = \Omega + \frac{mgr}{J_{\Sigma} \Omega}.$$

The block diagram of the proposed control algorithm is shown in figure 1.

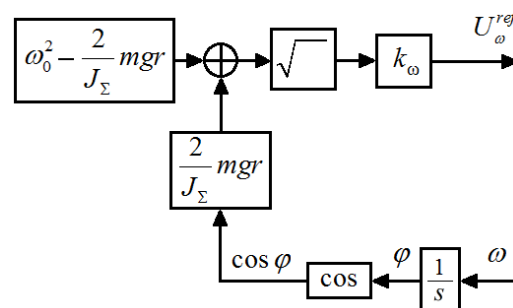


Figure 1. Block diagram of control algorithm for electromechanical unbalance vibration exciter.

Let us assume that the unbalance vibration exciter induction motor drive is a vector control system [8]. Current limitation in the system under study is provided by a current control loop. The block

diagram of the control system for the unbalance vibration exciter in view of the proposed control algorithm is presented in figure 2.

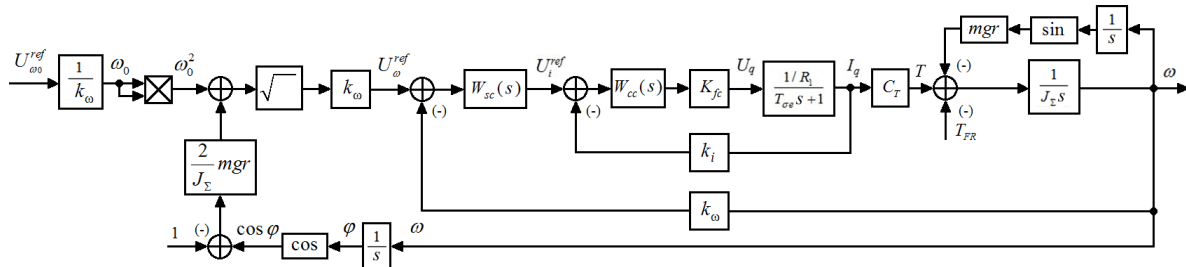


Figure 2. Block diagram of unbalance vibration exciter control system.

The following designations are used in figure 2: $U_{\omega_0}^{ref}$ – speed reference; $U_{\omega_0}^{ref} = k_{\omega}\omega_0$ – average speed reference; U_i^{ref} – current reference; U_q – q-axis primary voltage component; I_q – q-axis current component; k_{ω} – speed feedback coefficient; k_i – current feedback coefficient; $W_{sc}(s)$ – transfer function of the speed controller; $W_{cc}(s)$ – transfer function of the current controller; K_{fc} – transfer constant of the frequency converter; R_1 – ohmic resistance of the stator; $T_{\sigma e}$ – equivalent time constant of the stator’s circuit; C_T – proportionality constant expressing ratio of engine torque and q-axis current component.

The control system shown in figure 2 is represented as a single-channel control object, because it is assumed that the engine is a pre-magnetized one, and the flux linkage of the rotor equals to its rated value $\psi_2 = \psi_{2r}$. It is also considered that EMF in the quadrature axis control channel q e_q is compensated by the positive feedbacks [9].

The synthesis of the current controller was conducted in accordance with the accepted pass band of the current control loop:

$$\Omega_{ccl} \geq (6...10) \cdot \Omega .$$

The transfer function of the current controller was selected as follows [10]:

$$W_{cc}(s) = K_{cc} \frac{T_{\sigma e}p + 1}{T_{\sigma e}p},$$

where K_{cc} – transfer constant of the current controller given by:

$$K_{cc} = \frac{R_1 T_{\sigma e} \Omega_{ccl}}{K_{fc} k_i} .$$

The speed control loop was tuned to a technical optimum, and the time constant of the current control loop was accepted as a fast time constant [11]:

$$\tau_{\mu s} = \frac{1}{\Omega_{ccl}} .$$

The transfer function of the speed controller was selected as follows:

$$W_{sc}(s) = K_{sc} = \frac{J_{\Sigma} k_i}{2\tau_{\mu s} k_{\omega} C_T} .$$

4. Simulation results

Initial data for a design of the unbalance vibration exciter control system is an amplitude of the excitation force (A) and frequency of the excitation force (Ω): $A = 390000 \text{ N}$; $\Omega = 14\pi \text{ rad/s}$. Calculated and chosen parameters of the control system, which were being used in synthesis and modelling the system, are presented below.

Parameters of the eccentrics: rotation radius of the eccentric $r = 0.2 \text{ m}$; mass of the eccentric $m = 500 \text{ kg}$.

Parameters of the selected induction motor 4A280S10Y3: rated power – $P_r = 37 \text{ kW}$; rated phase voltage of the stator – $U_{1r} = 220 \text{ V}$; the rated number of revolutions – $n_r = 590 \text{ rev/min}$; rated engine torque – $T_r = 600 \text{ N}\cdot\text{m}$; rated phase current of the stator – $I_{1r} = 79 \text{ A}$; $C_r = 6.95 \text{ Wb}$; ohmic resistance of the stator $R_1 = 0.0835 \Omega$; the equivalent time constant of the stator's circuit $T_{\sigma e} = 24.24 \cdot 10^{-3} \text{ s}$.

The total inertia moment of the drive reduced to the motor shaft: $J_{\Sigma} = 23.6 \text{ kg}\cdot\text{m}^2$.

The transfer constant of the frequency converter: $K_{fc} = 31.1$.

Structured modeling of the synthesized control system for the electromechanical unbalance vibration exciter was carried out in the MATLAB/Simulink software package.

For a comparative assessment of the results, in addition to the synthesized control system, providing a free rotational movement (FRM), the cascade control system (CCS), having the same parameters of the power unit, has also been synthesized. The current control loop of each system was being tuned to the pass band $f_{ccl} = 70 \text{ Hz}$. The frequency converter was being represented as an instantaneous element. The speed control loop of each system was being tuned to a technical optimum. Speed reference U_{ω}^{ref} in the case of system, realizing FRM, corresponds to algorithm (1), at the same time $\omega_0 \approx \Omega$, but in the case of the cascade control system, speed reference is $U_{\omega}^{ref} = \Omega \cdot k_{\omega}$.

The simulation results are presented as the graphs of transient processes for each system. Transient processes of the eccentric's rotational speed are shown in figure 3, and transient processes of the q-axis current component are depicted in figure 4.

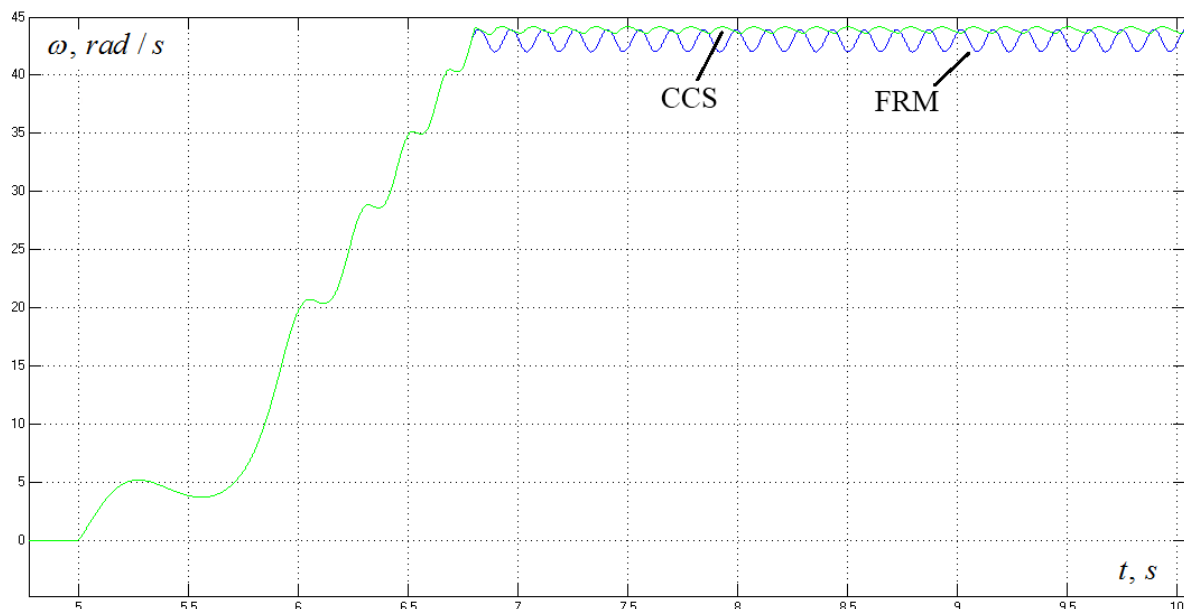


Figure 3. Transient processes of the eccentric's rotational speed $\omega(t)$.

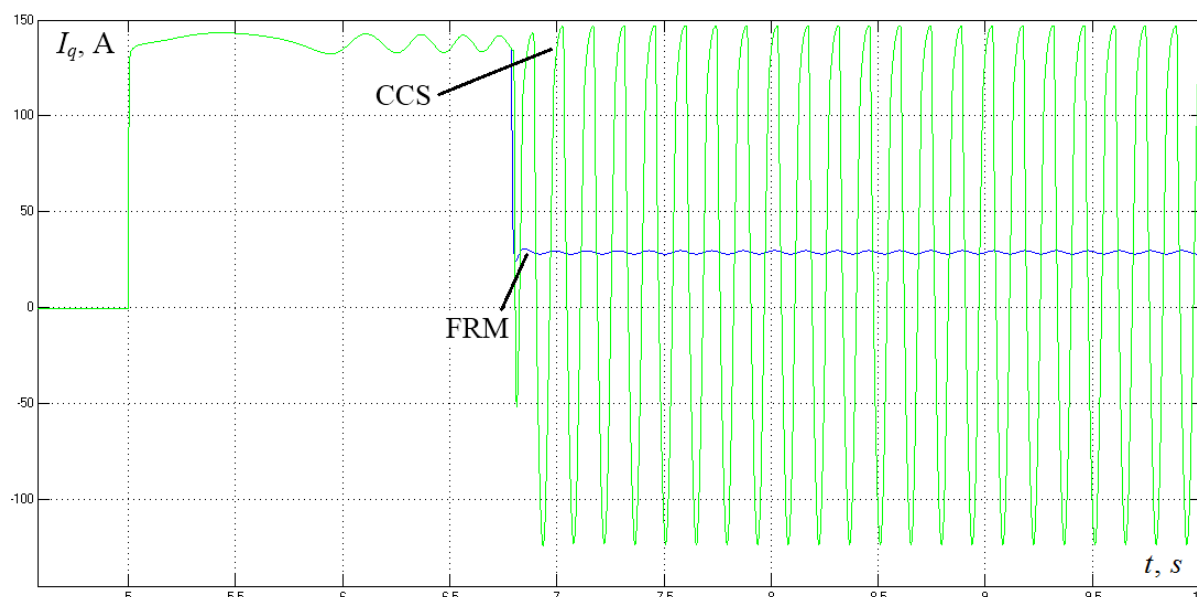


Figure 4. Transient processes of the q-axis current component $I_q(t)$.

5. Results and discussion

The comparison of the control system that provides FRM and CCS, having the same parameters of the power unit, has been carried out. From the analysis of transient processes, shown in figures 3 and 4, it can be argued that the amplitude of speed fluctuation does not exceed 5% of the reference value in the quasi-steady mode for both systems. While the amplitude of q-axis current component oscillation in the quasi-steady mode is 50 times less in the system, realizing FRM, compared with the one in the cascade control system.

In consideration of the fact that during electric drive acceleration, the dynamics of both systems are identical, one can talk about obvious advantages of the proposed control law compared with the constant speed reference.

6. Conclusion

The results obtained show the efficiency of the proposed control law in a limited frequency range. When removing the frequency of the generated seismic signal from its initial value Ω amplitude of speed fluctuation begins to increase and, hence, RMS of the excitation force starts to decrease.

However, when the electric drive is running at the speed corresponding to the initial value of the seismic signal, speed fluctuation is negligible, and the amplitude of the seismic signal corresponds to the required one.

Furthermore, it was found that the RMS of the stator phase current is 1.9 times less in the system, realizing FRM, in comparison with the one that takes place in the cascade control system. Hence, the copper loss of the induction motor is about 3.7 times less in the system with the proposed control law.

References

- [1] Potapenko M A 2008 *Journal of machinery manufacture and reliability* **37** 228–229
- [2] Skazka V V, Serdyukov S V and Kurlenya M V 2014 *Journal of mining science* **50** 1026–32
- [3] Tkach K B 1995 *Journal of mining science* **30** 68–73
- [4] Kichkar' I Y 2006 *Chemical and petroleum engineering* **42** 692–697
- Blekhman I I, Vasil'kov V B and Yaroshevich N P 2013 *Journal of machinery manufacture and reliability* **42** 192–195
- [5] Potapenko M A 2015 *Journal of machinery manufacture and reliability* **44** 319–323
- [6] Beenken W, Gock E and Kurrer K–E 1996 *Int. journal of mineral processing* **44–45** 437–446
- Jadot F, Malrait F, Moreno–Valenzuela J, Sepulchre R 2009 *IEEE Transactions on control systems*

technology **17** 646–657

[7] Romero M E, Seron M M, De Doná J A 2010 *IET Control theory and applications* **4** 1707–24

Potapenko E M and Potapenko E E 2007 *Journal of automation and information sciences* **39** 1–15

[8] Bondarko V A 2010 *Automation and remote control* **71** 1849–63